Title
SPARK CHAMBER USING HELIUM OR HYDROGEN AT HIGH DENSITY

Permalink
https://escholarship.org/uc/item/1zm070h0

Author
Schnurmacher, Gerald L.

Publication Date
1965-03-17

UCRL-16010 erratum

University of California

Ernest O. Lawrence Radiation Laboratory

SPARK CHAMBER USING HELIUM OR HYDROGEN AT HIGH DENSITY

Berkeley, California

UCRL-16010

UNIVERSITY OF CALIFORNIA
Lawrence Radiation Laboratory
Berkeley, California

AEC Contract No. W-7405-eng-48

July 13, 1965

ERRATUM

TO: All recipients of UCRL-16010
FROM: Technical Information Division
SUBJECT: UCRL-16010, Spark Chamber Using Helium or Hydrogen at High Density, Gerald L. Schnurmacher, March 17, 1965.

Please correct the subject report by interchanging Figs. 5 and 7. The existing legends are correct.

done

Nuclear Instruments and Methods

UCRL-16010

UNIVERSITY OF CALIFORNIA

Lawrence Radiation Laboratory
Berkeley, California

AEC Contract No. W-7405-eng-48

SPARK CHAMBER USING HELIUM OR HYDROGEN AT HIGH DENSITY

Gerald L. Schnurmacher

March 17, 1965

SPARK CHAMBER USING HELIUM OR HYDROGEN AT HIGH DENSITY

Gerald L. Schnurmacher

Lawrence Radiation Laboratory
University of California
Berkeley, California

March 17, 1965

Abstract

Efficiency data and threshold voltages are given for a four-gap helium spark chamber in which the pressure was varied from 1 to 30 atmos (gauge) while the voltage was varied from 13 to 30 kV. Data is also presented for the same spark chamber using unadulterated hydrogen gas up to 6 atmos pressure.

1. Introduction

In the past few years spark chambers have developed significantly to the stage that they now have joined the family of useful analytical techniques for high-energy-physics experiments at large accelerators. However, spark chambers as currently used still suffer from one major drawback in experiments where they are used in conjunction with liquid-hydrogen targets: they have not coexisted in the same spatial volume. As a result, it is difficult to locate precisely the origin of interactions taking place in the hydrogen target, and the data obtained is complicated by scattering off the walls of the hydrogen vessel. These disadvantages could be eliminated by placing liquid-hydrogen wafers inside the plates of the chamber, or better yet, by immersing the plates in liquid hydrogen[1]. With this in mind, two experiments were undertaken, the results of which are presented here.

The first experiment, represented by 11,000 analyzable pictures, determined the feasibility of making a low-temperature gaseous-helium spark chamber utilizing hollow plates filled with liquid hydrogen. For this experiment a small high-pressure chamber was designed in which the helium could be raised to the appropriate pressure to give a density that would correspond to the density resulting from the low temperature provided by liquid hydrogen.

In the second experiment unadulterated hydrogen gas was used in place of helium in the hope that the performance at the densities attainable from pressurizing the hydrogen would be a starting point toward ultimately determining the feasibility of sparking in liquid hydrogen. A possible alternative to a liquid-hydrogen chamber would be one using pressurized gaseous hydrogen at low temperature to obtain a density approaching that of the liquid. Because of the high-voltage threshold requirements for hydrogen, the equipment used was not adequate to give an average gap efficiency greater than about 68% at moderate pressure. The data presented should be of benefit in future investigations, and new equipment is currently being built to enable the study at higher pressure to continue.

2. Experimental Method

2.1. DESIGN OF CHAMBER AND RUNNING CONDITIONS

The spark-chamber vessel and plate assembly used in both experiments is shown in fig. 1. The spark-chamber plates were fabricated from 1/2-inch-thick aluminum stock and were 32 square inches in area. Four 0.125-inch gaps were used in order to give adequate track definition, and all runs were made with cosmic rays.

In the helium experiment the chamber vessel was pumped down to a few microns and flushed with helium three times before beginning the initial run. Thereafter, throughout the course of the experiment, the helium was changed every 2 to 4 hours, and in cases where the chamber was not pulsed for several hours, it was always flushed three times before beginning a run. By this method, gas contamination inside the chamber was kept at a minimum. In the hydrogen experiment, a similar technique was followed.

2.2. DETECTION AND TRIGGER SYSTEM

The electronics are shown diagramatically in fig. 2. The chamber was triggered by a threefold scintillator coincidence pulse. The scintillators, coupled to RCA 6810A photomultiplier tubes by means of a light pipe, were arranged in a vertical geometry above and below the chamber such that their solid angle coincided with the size of the spark-chamber plates and limited the trigger pulses to cosmic rays that were nearly vertical. The output of the threefold coincidence circuit was used to drive a 10-Mc discriminator circuit which had parallel outputs to a scaler and a gating circuit. If the camera had recycled and the time required for the power supply to recharge had elapsed, the gating circuit gave out a pulse which triggered a 10-Mc discriminator. This pulse in turn had parallel outputs to a scaler and a 5-kV hydrogen thyratron prepulser[2] which was used to trigger a spark gap[2] which in turn fired the chamber by discharging a 2000-pF coupling capacitor. In later runs, a 5000-pF coupling capacitor was used. This increase in coupling capacitance did not appear to affect the operation of the chamber. For the initial runs at 16 kV and below, a spark gap was used. Since the chamber capacitance was less than 10^3 pF [3], it was decided after the first 40 runs to replace the spark gap with a 30-kV pulser[4] utilizing a Kuthe 5949 hydrogen thyratron, which was used in all runs above 16 kV. This pulser eliminated the necessity of having to readjust the spark-gap spacing as a function of the voltage used. The second and fourth plates of the chamber received the negative high-voltage pulse, whereas the first, third, and fifth plates were connected to ground through a copper strip.

Since the experiment was done with cosmic rays and the camera had a 300-ms recycling time, it was felt unnecessary to use a clearing field. Delay time between the prepulser trigger and the main high-voltage pulse was limited to a maximum of about 100 nsec to insure good operation of the chamber.

3. Data Recording and Analysis

Data was recorded with an electronically pulsed 35-mm Beattie-Coleman camera placed 6 feet from the chamber. The camera looked through a 2-inch-thick lucite window comprising the front of the chamber. The camera was pulsed, and a picture was recorded on DuPont 140B film every time the chamber fired. Approximately 15,000 pictures were recorded for both the helium and hydrogen experiments.

Each picture was scanned and the data recorded on IBM cards. A 7094 computer program was written, and 272 parameters were calculated for each of the 114 discrete pressure-voltage runs. The efficiencies for each gap as well as the average four-gap efficiency were among the many parameters calculated. The efficiency data covers the pressure range from 1 to 30 atmos and the voltage range from 13 to 30 kV. Approximately 130 to 230 pictures were taken for each discrete pressure-voltage run. We define the individual gap efficiencies as

$$\epsilon_A = \frac{N_{tot}(ABCD)}{N_{tot}(BCD)+N_{tot}(ABCD)} , \tag{1}$$

$$\epsilon_B = \frac{N_{tot}(ABCD)}{N_{tot}(ACD)+N_{tot}(ABCD)} , \tag{2}$$

$$\epsilon_C = \frac{N_{tot}(ABCD)}{N_{tot}(ABD)+N_{tot}(ABCD)} , \tag{3}$$

and

$$\epsilon_D = \frac{N_{tot}(ABCD)}{N_{tot}(ABC)+N_{tot}(ABCD)} , \tag{4}$$

where A, B, C, and D are the individual gaps from top to bottom of the chamber, $N_{tot}(ABCD)$ is the number of tracks in a discrete pressure-voltage run where all four gaps fired, and $N_{tot}(BCD)$ is the total number of tracks in a discrete pressure-voltage run where gaps B, C, and D fired and gap A did not. The average four gap efficiency was calculated from

$$\bar{\epsilon} = \frac{\epsilon_A + \epsilon_B + \epsilon_C + \epsilon_D}{4} , \qquad (5)$$

where ϵ_A, ϵ_B, ϵ_C, and ϵ_D are given in eqs. (1) through (4).

4. Results and Interpretation

4.1. HELIUM

There is confirming experimental evidence showing that a 1-atmos helium spark chamber does not work as efficiently as a chamber utilizing argon or neon. This is a result of helium having only about eight ion pairs per atmos-cm for minimum-ionizing particles, which is much less than that for one of the aforementioned noble gases. However, by increasing the pressure in a helium chamber, the efficiency can be increased as the number of ion pairs increases, but the threshold voltage also increases with pressure (fig. 3). Because the efficiency is influenced strongly by the degree of overvoltage (with respect to threshold), for a constant voltage the efficiency should increase with increasing pressure until the degree of overvoltage is too low. At this point the voltage must be increased to maintain the efficiency. The 90% efficiency line in helium as a function of voltage and pressure is shown in fig. 4.

Average gap efficiencies for helium at pressures from 0 to 300 psig and 13, 15, and 17 kV, using a spark gap, are shown in fig. 5, a, b, and c, respectively. The average gap efficiency at 28 kV using a hydrogen thyratron pulser and covering the pressure range from 150 to 450 psig is shown in fig. 6.

Very few frames in the runs plotted in fig. 5 contained multiple-track events. (As used here, a frame is the area of film exposed by each triggering of the spark chamber, a single-track event is three or four sparks whose centers lie on a straight line. Multiple-track events are defined as events resulting in more than one track per frame. These events presumably are due to electron showers.) Consequently, when the efficiency for single-track events was compared with that for all events (single- and multiple-track events), the two were found to be identical within the systematic and statistical errors of the experiment. In these runs an increase in the voltage resulted in expanding the width of the efficiency peak on the high-pressure side but not significantly increasing the maximum efficiency. This follows the prediction from the pressure-overvoltage relationship discussed previously. A maximum efficiency of 94 to 98% at 13, 15, and 17 kV was reached at approximately 90 psig. Figure 6 shows that if the degree of overvoltage above threshold is great enough, near maximum efficiency can be maintained over a fairly wide pressure range. In the runs plotted in fig. 6, there were more frames found that contained multiple-track events than were present in the 13-, 15-, and 17-kV data. As a result, when the single-track event efficiency at 28 kV was compared with the efficiency for all events in these runs including those with greater than one track, approximately a 5% difference was found as fig. 6 shows. No explanations were found for this increase in the number of multiple-track events at higher voltage and pressure.

In the runs plotted in fig. 5, only one high-voltage lead was used, and no attempt was made to decouple the plates electrically. In addition there was a ±0.004-in. variation in gap spacing. Both of these factors contributed a deleterious effect to chamber efficiency particularly at pressures above 150 psig. In the runs plotted in fig. 6, gap spacing was corrected to ±0.001 inch, and an attempt was made to decouple the high-voltage plates electrically by running in separate high-voltage leads in parallel and installing 10-ohm Globar resistors in series. This greatly improved the efficiency of the chamber. The contribution of gap spacing, which was originally greatest in gap B, is reflected in fig. 7, which is the individual-gap efficiency plot at 17 kV, covering the pressure range from 15 to 300 psig. As can be seen from fig. 7, nonuniformity of gap spacing decreases individual gap efficiency by 2 to 20% at 40 to 150 psig, and at 180 to 300 psig the effect is most severe, lowering the individual gap efficiency 43 to 70%. Figure 8 is the plot of individual gap efficiency at 28 kV corresponding to fig. 6. It shows how individual gaps behave after the chamber electrodes were regapped and the high-voltage leads decoupled. No explanation could be found for the poor behavior of gap A in these runs. The gap spacing in gap A was not the widest. Figure 9 shows the efficiency of gap A for single-track events only and multiple-track events only, and illustrates the effect of multiple-track events on a bad gap.

Throughout the runs, gap robbing in both single and multiple-track events proved to be a significant problem. Since the value of the coupling capacitor was only 5×10^3 pF, the first track to form presumably used up most of the energy. This resulted in very faint and inefficient tracks for charged particles that passed through the chamber latest in time. Another effect of gap robbing was noticed in single-track events, where one gap often did not fire at all, and at other times sparks in one or two gaps were at least an order of magnitude fainter than the other sparks in the track. This latter case of sparks of different intensities within the same track creates somewhat of a problem in data recording when the photographic technique is used. If the camera lens iris is opened up to record the faint sparks, the brighter ones are greatly overexposed and appear as wide blobs with large halos. If the iris is stopped down to get a sharp image of the bright sparks, the faint ones are not recorded. In some of the frames analyzed, particularly those at higher pressures, spurious sparking was common. In the future this condition can perhaps be circumvented by the use of alcohol vapor, which acts as a quenching agent, absorbing ultraviolet light and thereby limiting the number of secondary electrons from photoemission. Alcohol also decreases halo size and sharpens up the sparks[5]. Cap robbing and the resultant loss of efficiency in multiple-track events can usually be overcome by the use of a larger discharge capacitance. This increases the discharge time of the coupling capacitor, thereby providing energy for the discharge for particles that passed through the chamber later in time. Increasing the coupling capacitance, however, has the disadvantage of broadening the sparks, which were wider than normal anyway. The widening of the sparks appeared to be worst at the higher pressures, but perhaps the use of a small amount of alcohol vapor as previously suggested would circumvent this widening effect at high pressure. If this effect cannot be overcome, some compromise in capacitance increase and resulting multiple-track efficiency must be made to maintain narrow sparks and good resolution.

4.2. HYDROGEN

Hydrogen has less than four ion pairs per atmosphere-centimeter for minimum ionizing particles compared to approximately eight in helium, about 25 in neon and about 40 in argon. Therefore, if hydrogen is used as an environmental gas, it is necessary to attain sufficient density by gas pressurization, thereby providing enough ion pairs for the discharge mechanism to be initiated. From the work done, it is predicted that the minimum gas pressure required for high efficiency operation should be in the order of 30 atmos. If a sufficient amount of voltage above threshold is used, it is presumed that an efficiency of 90% or better could be attained. At this pressure and room temperature, the density of the gas is still only about 1.3×10^{-3} g/cm^3 compared to 70×10^{-3} g/cm^3 for hydrogen in the liquid state at 1 atmos. The main purpose of the tests in gaseous hydrogen was to search for unusual effects as gas density was varied and to determine threshold breakdown voltages as well as the voltages required for reasonable efficiency$^{6)}$.

As the maximum voltage of the power supply and pulse equipment used for both the helium and hydrogen experiments was only 30 kV, the results presented for hydrogen are somewhat limited. Approximately 3400 useful pictures were taken and analyzed for various parameters. The data presented covers the pressure range from 0 to 90 psig at voltages to 29 kV.

A plot of the breakdown-threshold voltage in hydrogen using solid aluminum electrodes and a 0.125-inch gap spacing is shown in fig. 10. As indicated by the graph, the threshold voltage rises very rapidly with increasing pressure, and at 90 psig, 29 kV is below breakdown threshold. At this latter pressure there are still not enough ion pairs available to initiate breakdown consistently. The results for low pressure and density conditions are presented in fig. 11. Figure 11a shows the average four-gap efficiency for single-track events only at 28 kV. The maximum efficiency attained at this voltage was 48% at 30 psig. Figure 11b is a plot of the average four-gap efficiency for single-track events at 29 kV and shows that the maximum efficiency reached was 68% at 30 psig. In comparing this maximum with that shown in fig. 11a, the effect of overvoltage (above threshold) can be seen. The maximum efficiency for single-track event frames at 29 kV (fig. 11b) is shown to be somewhat higher (about 5%) than that for all events including those with greater than one track at the same voltage (fig. 11c). This effect is consistent with the results found in helium. Presumably the effect is due to gap robbing and the size of the coupling capacitance. In fig. 11c at 29 kV and 45 psig, 11% of the frames contained three-gap tracks; however, since no four-gap tracks were present, the efficiency as defined above is zero. As the pressure is increased, and voltage held constant at 29 kV, the number of three-gap tracks decreases and the number of one- and two-gap "tracks" increases, again illustrating the voltage dependency of the chamber.

In hydrogen, the fraction of the total number of frames analyzed that had a three- or four-gap track plus a two-, three-, or four-gap "track" varied from 4% to 42%, while the average was 25%. Table 1 shows the percentage of the total number of frames having three- and four-gap tracks in frames having 1 to 6 tracks per event. The table covers the pressure range from 0 to 55 psig and voltages from 26 to 29 kV. It is evident from the table that the number of three- and four-gap tracks decreases with an increasing number of tracks per event. This shows that the greater the number of simultaneous tracks, the greater the degree of gap robbing and the lower the efficiency. As efficiency goes down, the number of gaps firing goes down, and it becomes difficult to separate real tracks from spurious sparks.

As in helium, the quality of the photographs in hydrogen was not very good because of severe differences in spark intensity from one gap to another. This again resulted in overexposing the brighter sparks in order to record the fainter ones, with the consequence that some of the sparks are very wide and have halos, while others range from normal intensity to barely visible. Figure 12 is a typical single-track event illustrating the aforementioned variation in spark intensity from one gap to another. The conditions in the chamber for fig. 12 were 30 psia and 29 kV. The camera lens iris was set at f/4 and the camera was located 6 feet from the chamber. In many of the pictures taken the spark intensity variation was considerably greater than that shown in fig. 12. Throughout the runs, the brighter sparks were not confined to any specific gap but were random with respect to gap preference, which excluded the possibility that this effect could be due to gap-spacing variation. The heterogeneity in intensity was found to be more prevalent in hydrogen than in helium and the effect is amplified as the number of gaps firing decreases.

5. Conclusions

Helium gas at liquid-hydrogen temperature (20.4°K) and 1 atmos has a density of about 2.5×10^{-3} g/cm^3. This density at room temperature (299.4°K) can be attained by pressurizing the gas to approximately 15 atmos. At this pressure the efficiency of the helium chamber described in this experiment was 90 to 95% using 28 kV of applied voltage. It is therefore concluded that it is feasible to build an efficient hollow-plate spark chamber using liquid-hydrogen wafers and low-temperature helium as the environmental gas. It is hoped that further study will prove the practicability of making a chamber where the electrodes can be immersed in liquid hydrogen.

6. Future Experiments and Improvements

Plans are underway to continue studies using hydrogen as the environmental gas. It is hoped that higher pressure can be employed with good efficiency by the use of higher-voltage equipment. Utilization of solid or foil plates produces a prohibitive voltage requirement, but this problem can be lessened by the adoption of wire electrode planes, which provide a higher local electrical field gradient per unit of applied voltage. Wire plates also have the additional advantage of creating local decoupling, which should aid in minimizing gap robbing. Further decoupling, ensuing from the use of separate high-voltage leads for each plate and decoupling resistors in series, is a necessity. A large coupling capacitance is also desirable if high multiple track efficiency is required. The effect of unequal gap spacing is considerable, and care should be taken to maintain close gap tolerances. The use of alcohol vapor mixed with the gaseous hydrogen should also be beneficial in eliminating spurious sparks, thereby decreasing gap robbing.

7. Acknowledgments

The author is particularly indebted to Dr. William Wenzel who suggested the experiment and offered many helpful suggestions and discussions throughout the course of the study. Thanks are also due the many people who contributed to the final results presented herein. I especially wish to thank Robert Miller who assisted in taking data, James Hebel who wrote the computer program, and Maria Remenyi who assisted in the data reduction. This work was done under the auspices of the U. S. Atomic Energy Commission.

Table 1

Percent of three- and four-gap tracks in hydrogen as a function of the number of tracks per frame.

Tracks per frame	Gaps firing per track	Percent of total frames
1	3	13.0
1	4	1.91
2	3	5.61
2	4	0.52
3	3	1.60
3	4	0.25
4	3	0.39
4	4	0.06
5	3	0.06
5	4	0.03
6	3	0.06
6	4	0.06

FOOTNOTES AND REFERENCES

1) E. F. Beall and V. Cook, Spark Chamber Tests at Low Temperature, Lawrence Radiation Laboratory Internal Report UCID-2401, November 1962 (unpublished work). These authors have studied the feasibility of such a spark chamber by running efficiency tests using helium at liquid-nitrogen temperature.

2) W. A. Wenzel, "Spark Chambers," in Annual Review of Nuclear Science (Annual Reviews, Inc., Palo Alto, California, 1964), Vol. 14.

3) In order to maintain a pulse rise time of $\sim 10^{-8}$ sec utilizing a single Kuthe 5949 hydrogen thyratron, the chamber capacitance must be less than 10^3 pF.

4) Preliminary unpublished work by H. M. Steiner of this laboratory using a pressurized-helium spark chamber indicated that the required voltages should not exceed 30 kV.

5) T. Elioff, Lawrence Radiation Laboratory, private communication.

6) The only previous work found in the literature dealing with a hydrogen spark chamber, [G. K O'Neill, Rev. Sci. Instr. (1961) 32, 528] contains no quantitative data on voltage requirements or efficiency.

Figure Legends

Fig. 1. Spark-chamber vessel and electrode assembly.

Fig. 2. Electronics block diagram.

Fig. 3. Threshold voltage in helium as a function of pressure. A thyratron pulser produced the high voltage.

Fig. 4. Ninety-percent-efficiency plot in helium as a function of voltage and pressure.

Fig. 5. Average-gap efficiency in helium at (a) 13 kV, (b) 15 kV, and (c) 17 kV, using a spark gap.

Fig. 6. Average-gap efficiency in helium at 28 kV, using a hydrogen thyratron pulser.

Fig. 7. Individual-gap efficiency in helium at 17 kV, using a spark gap.

Fig. 8. Individual-gap efficiency plot in helium at 28 kV, using a thyratron pulser.

Fig. 9. Efficiency of gap A for single and multiple-track events in helium at 28 kV.

Fig. 10. Threshold voltage in hydrogen as a function of pressure.

Fig. 11. Average gap efficiency for single-track events at (a) 28 kV and (b) 29 kV, and (c) all events at 29 kV in hydrogen.

Fig. 12. Four-gap track in hydrogen showing the difference in individual gap spark intensities.

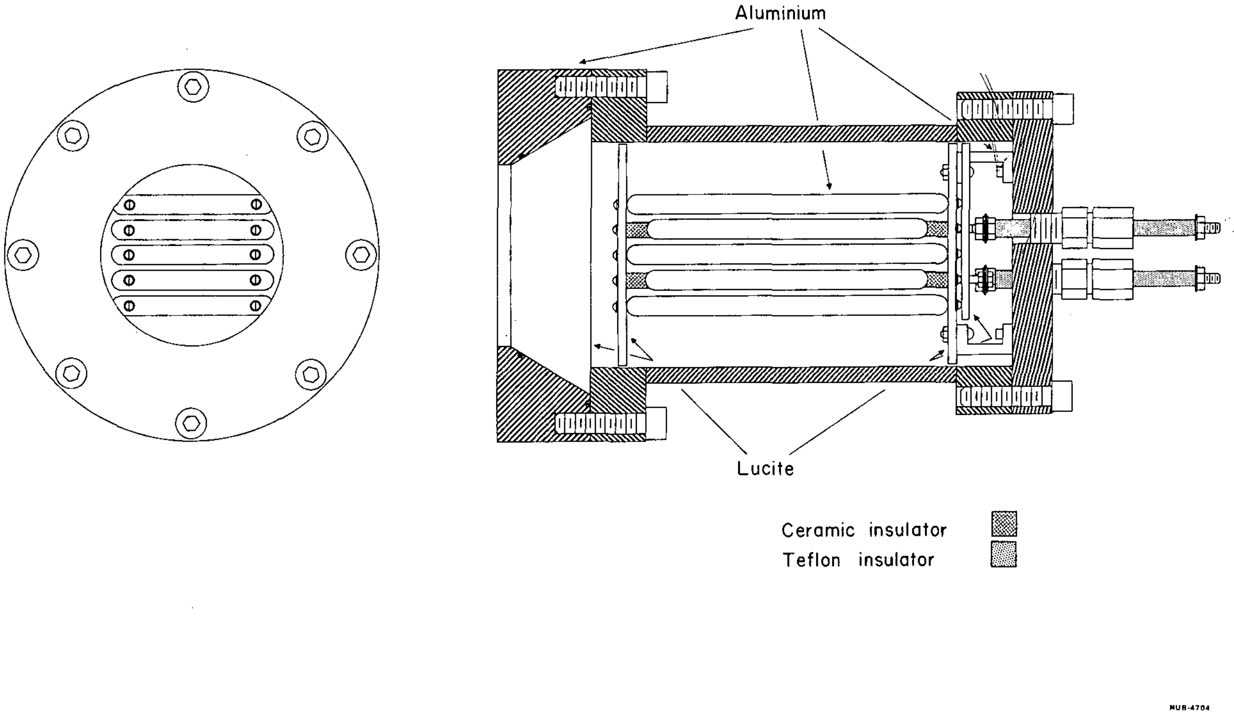
Aluminium
Lucite
Ceramic insulator ▨
Teflon insulator ▨
MUB-4704

Fig. 1

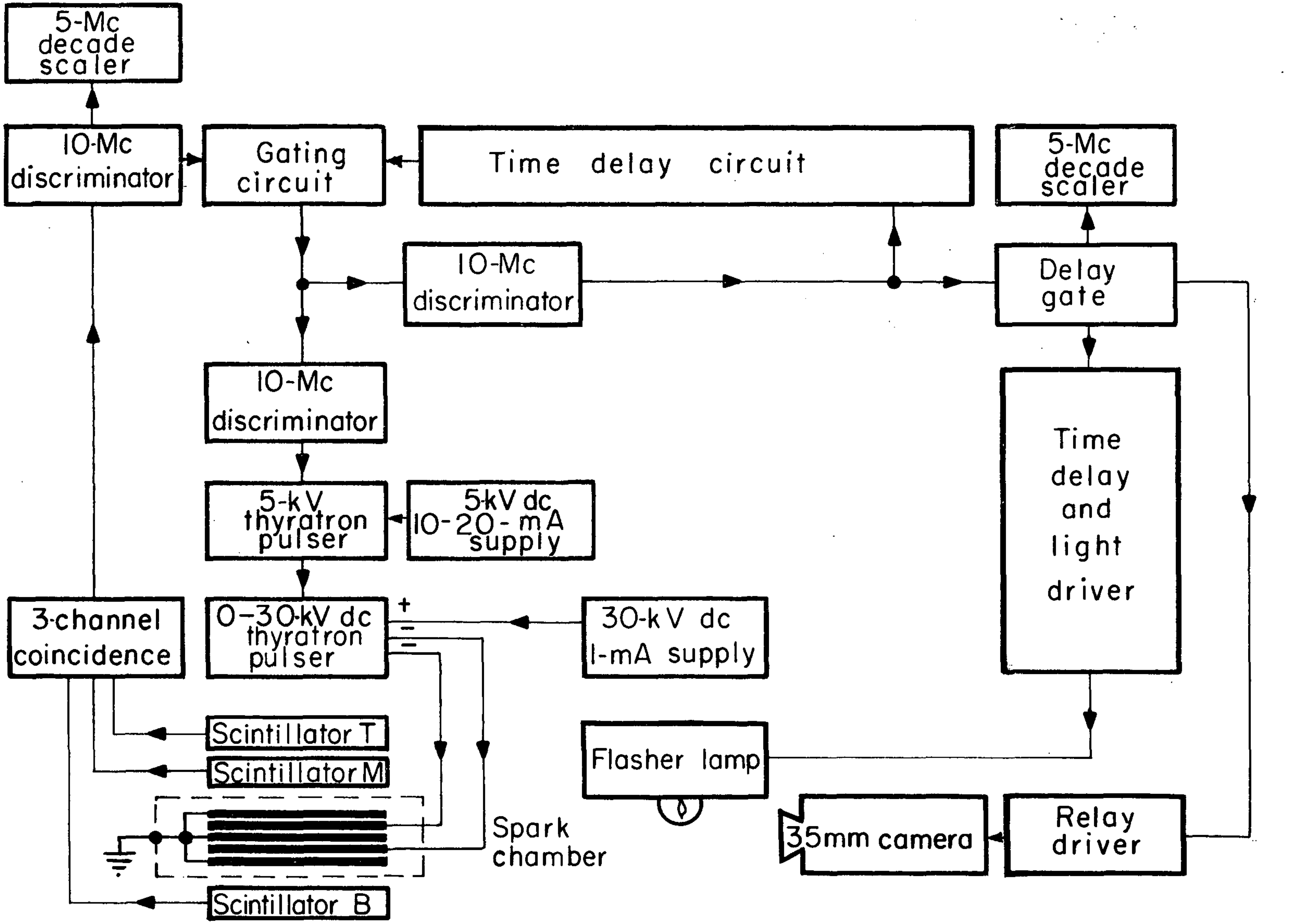

MUB-4703

Fig. 2

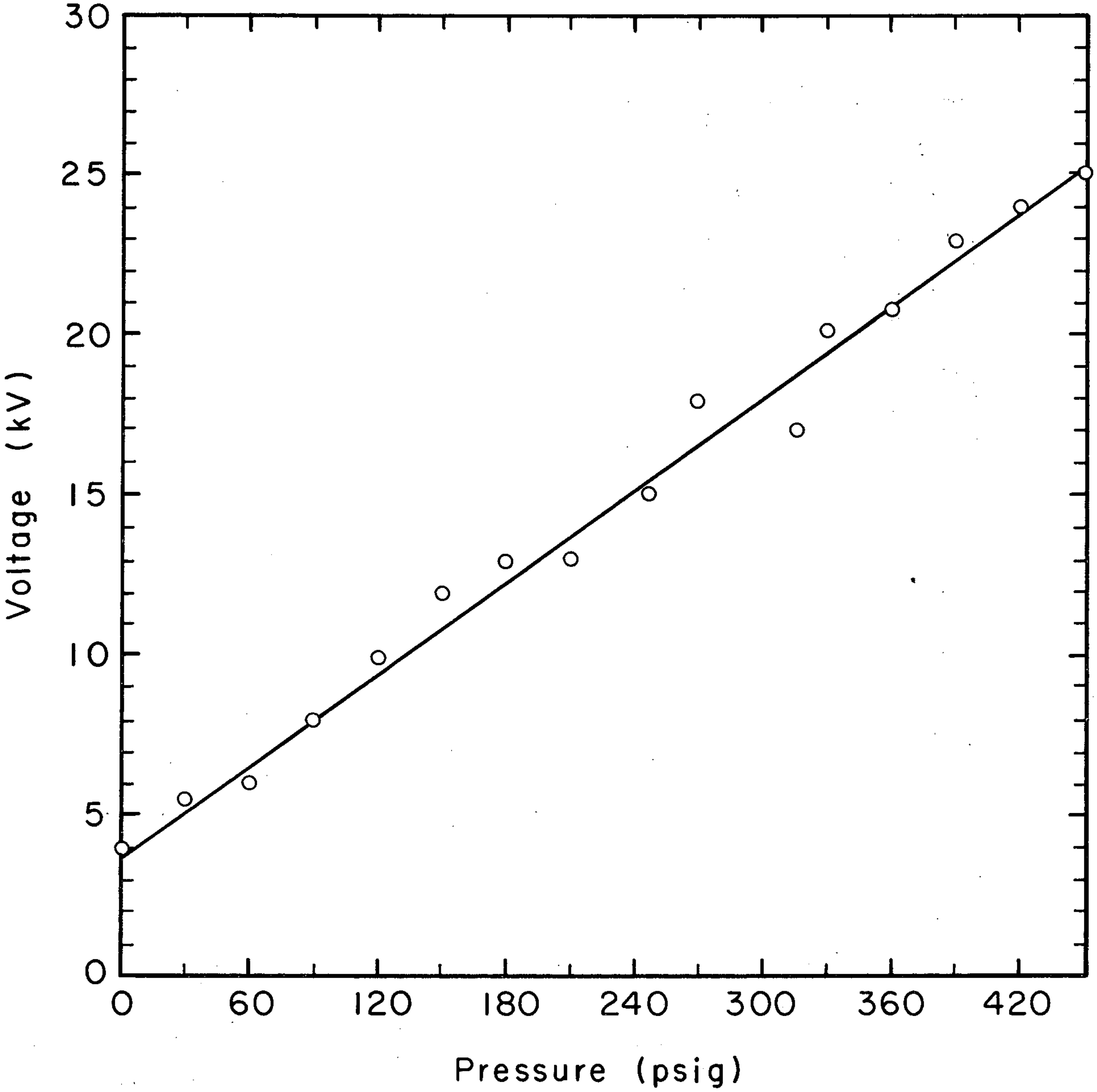

MUB-5678

Fig. 3

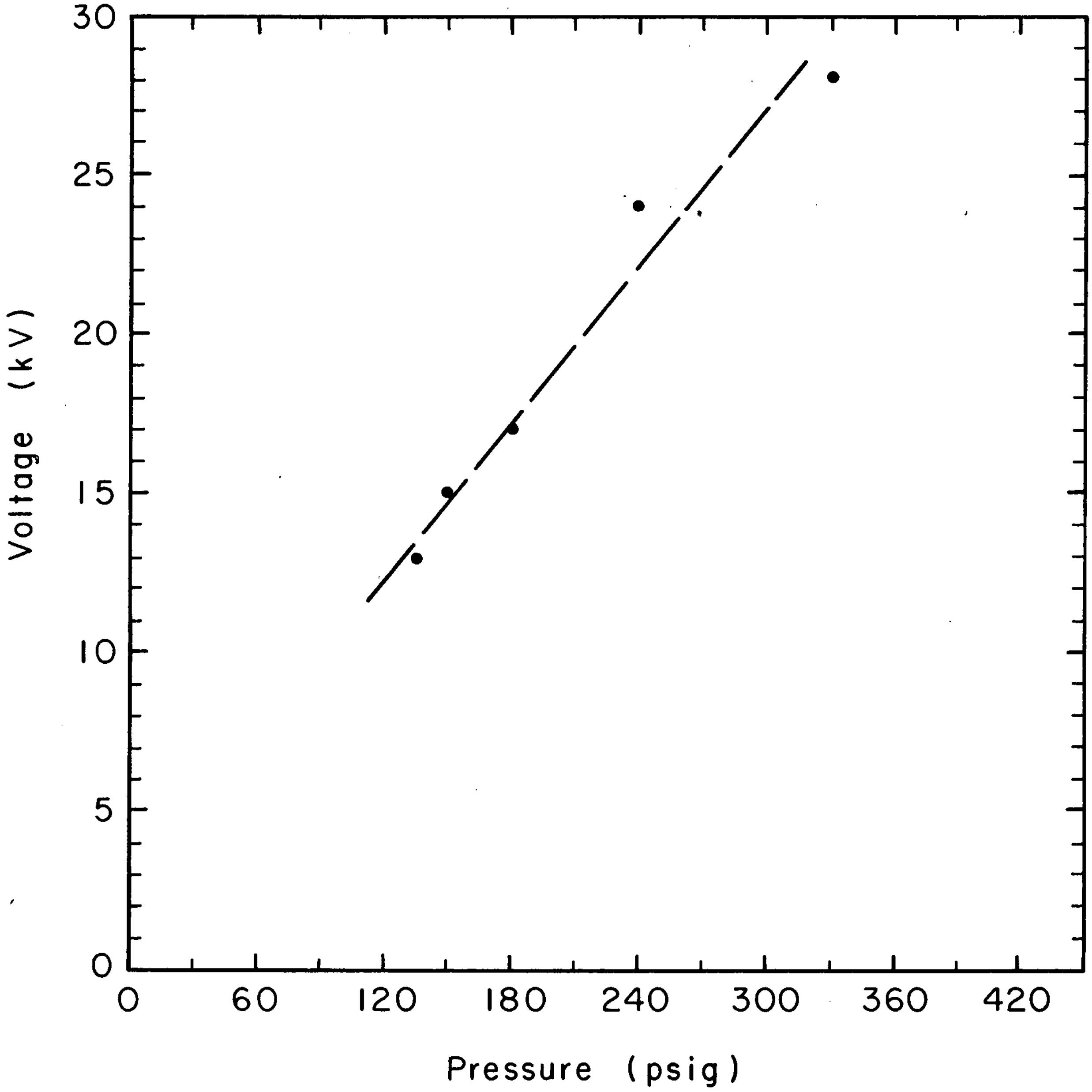

MUB-5679

Fig. 4

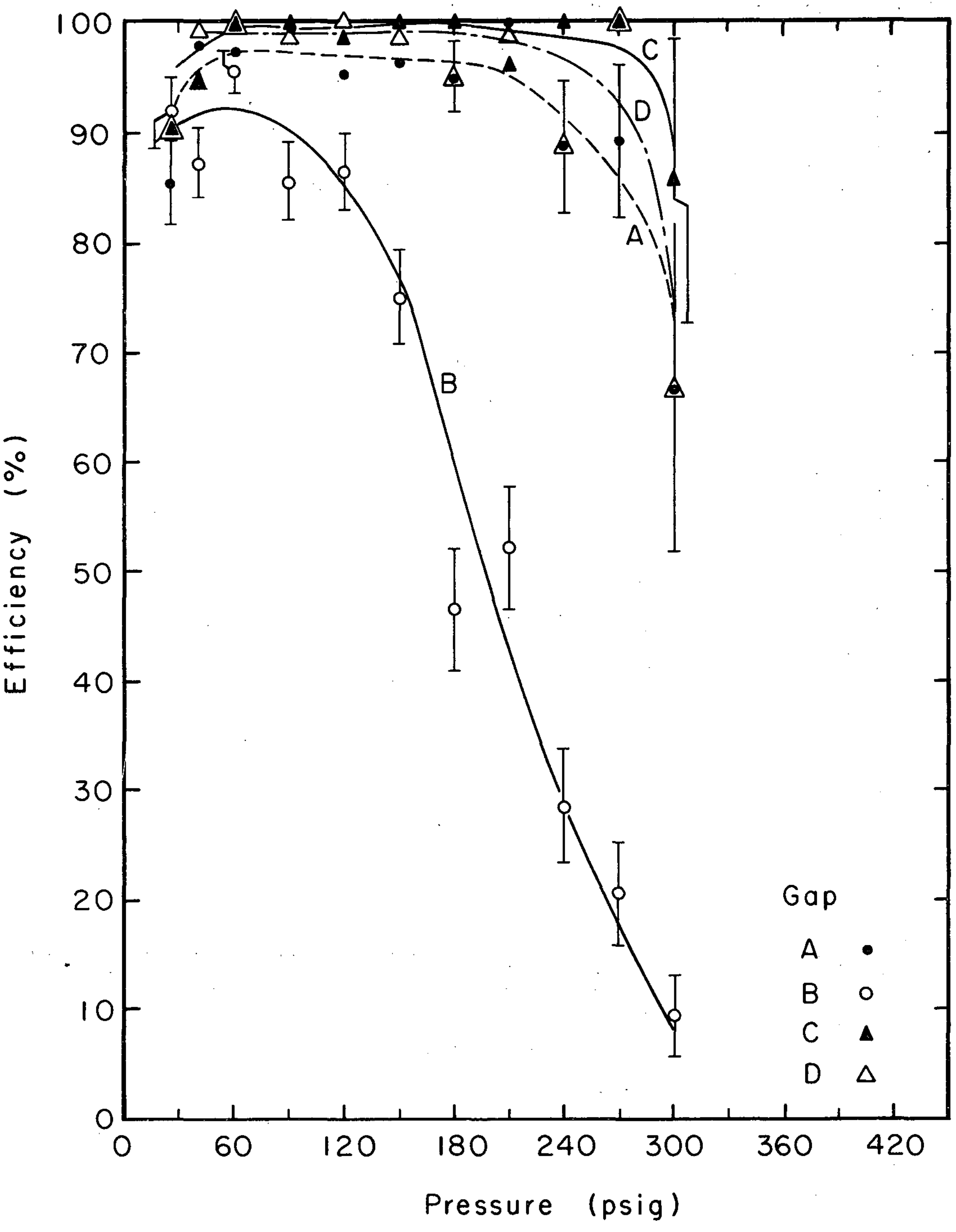

MUB-5680

Fig. ~~5~~ 7

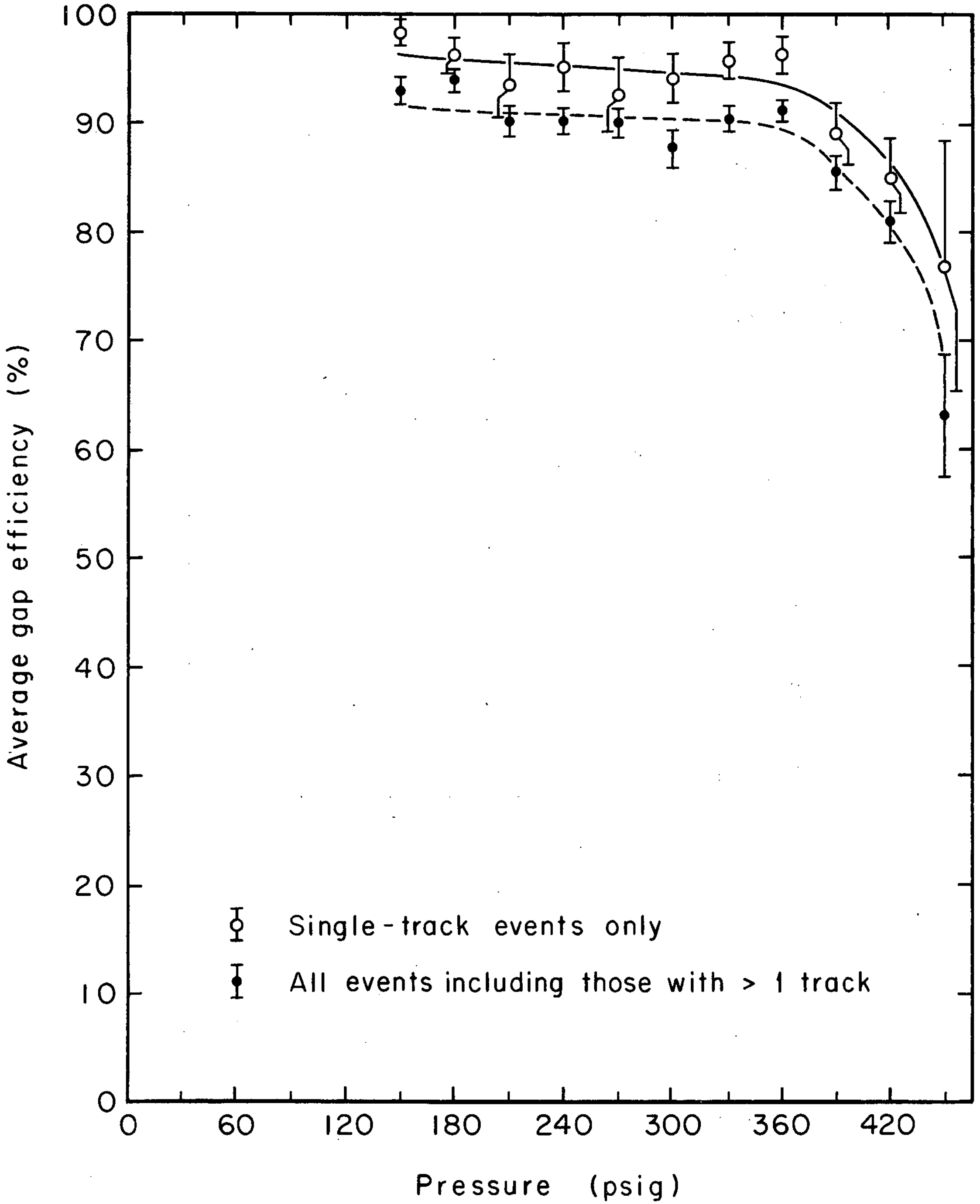

MUB-5681

Fig. 6

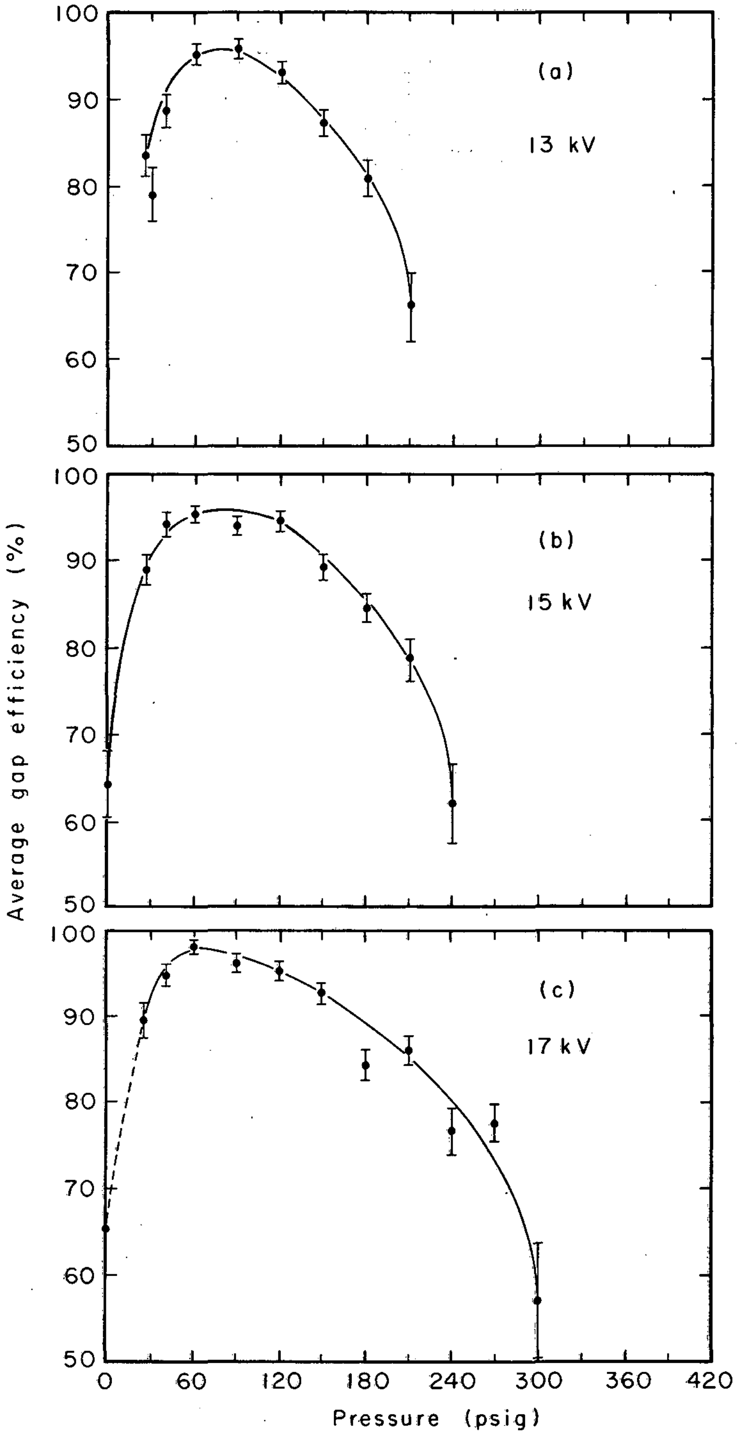

MUB-5682

Fig. 5

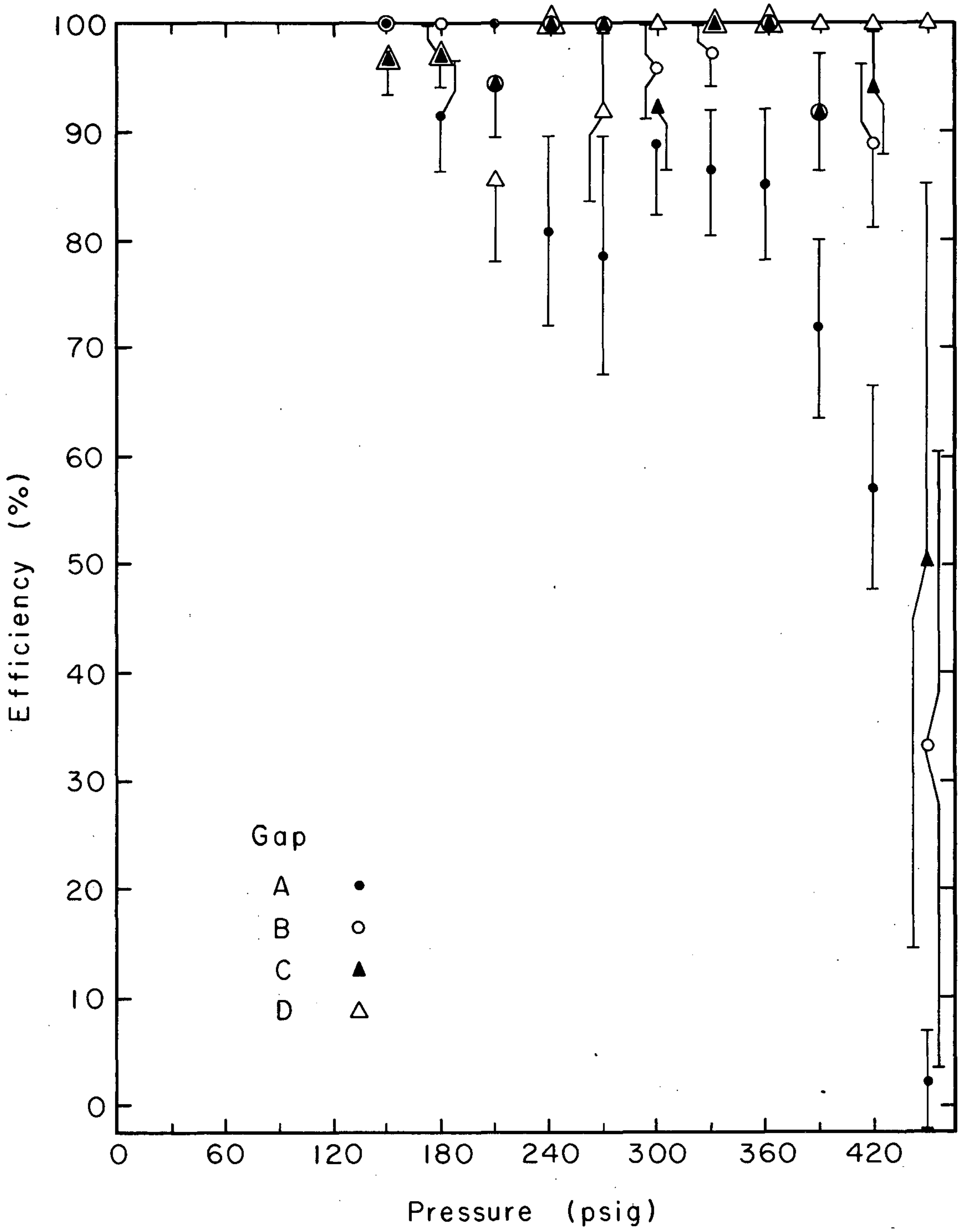

MUB-5683

Fig. 8

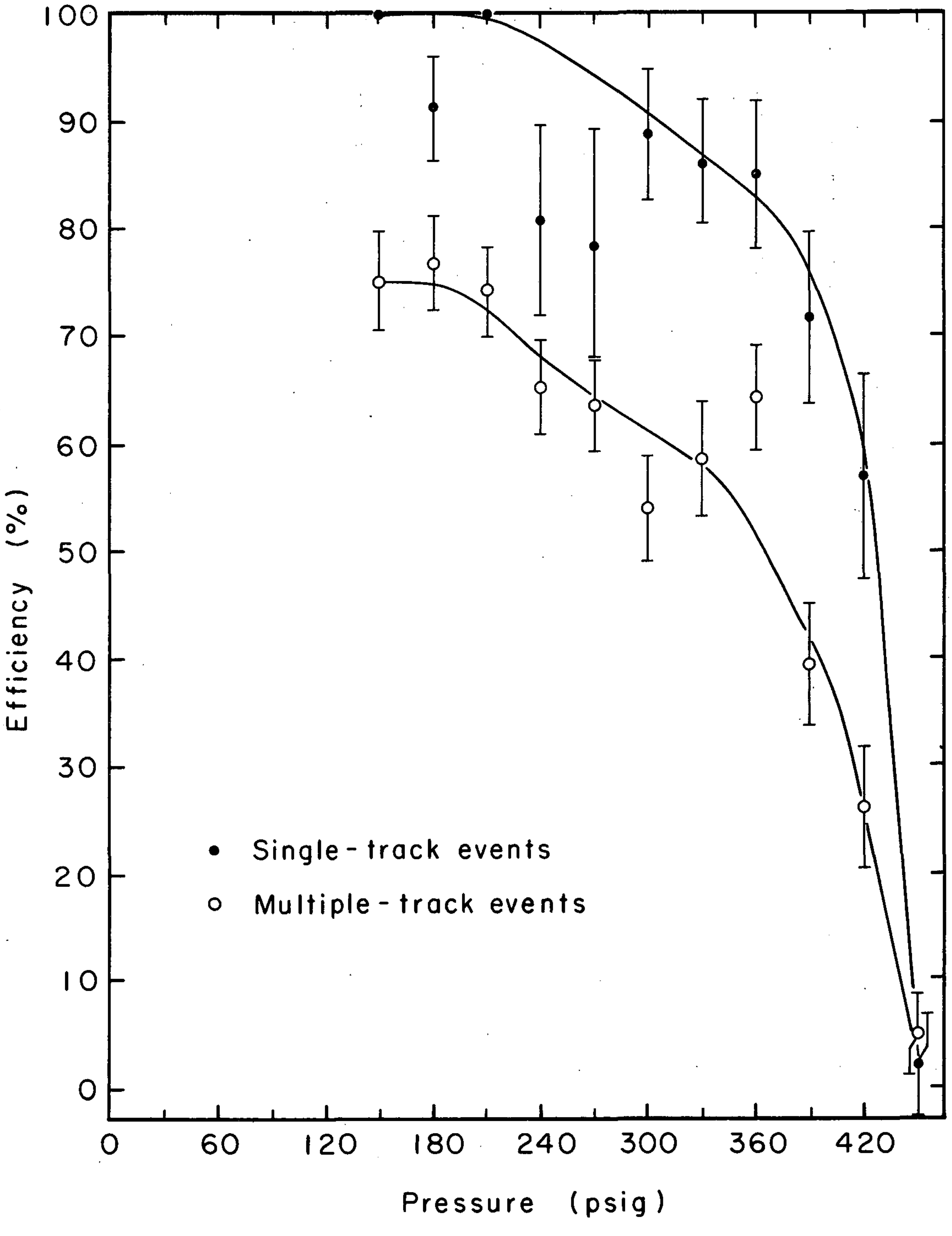

MUB-5684

Fig. 9

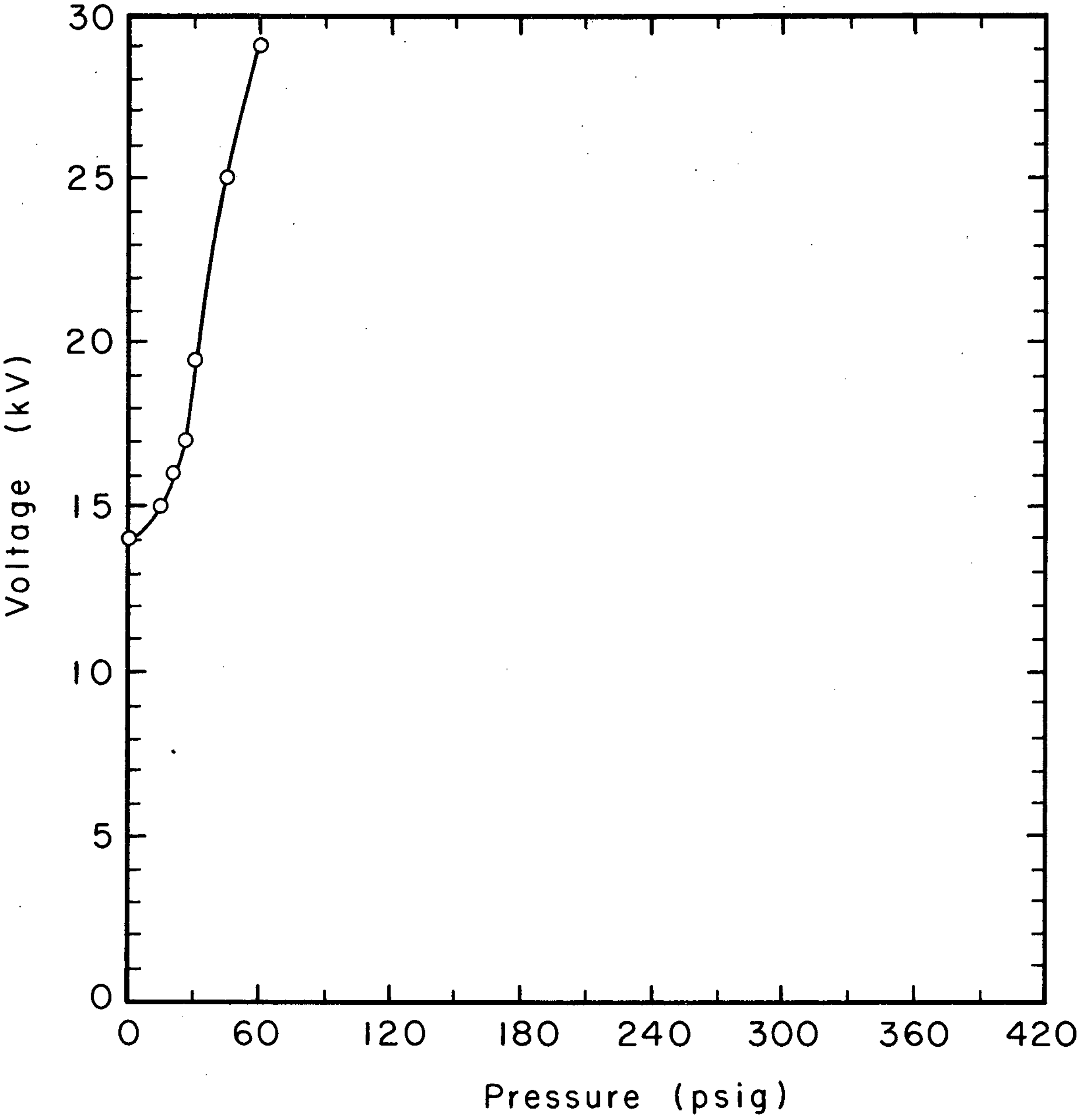

MUB-5685

Fig. 10

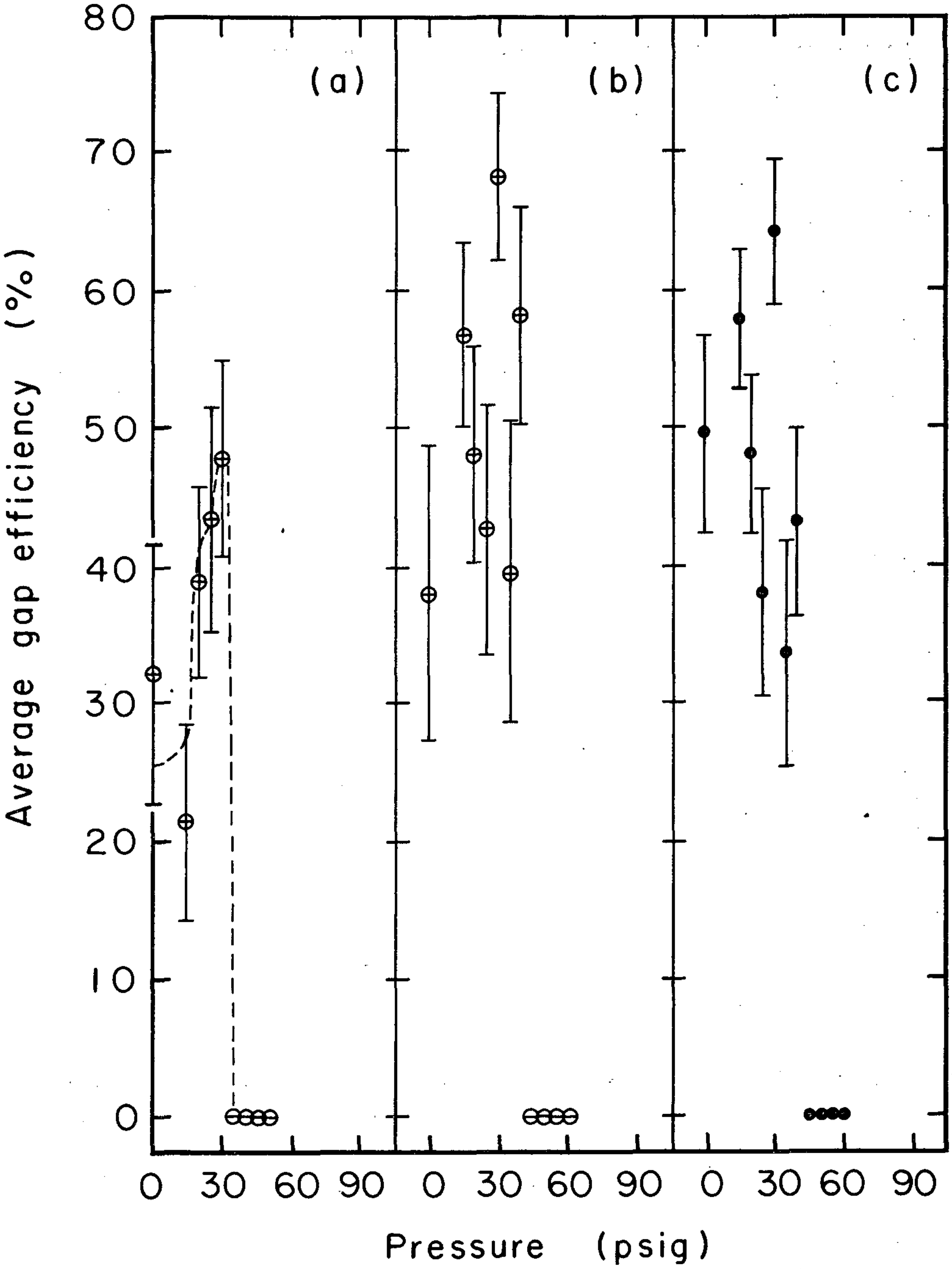

MUB-5686

Fig. 11

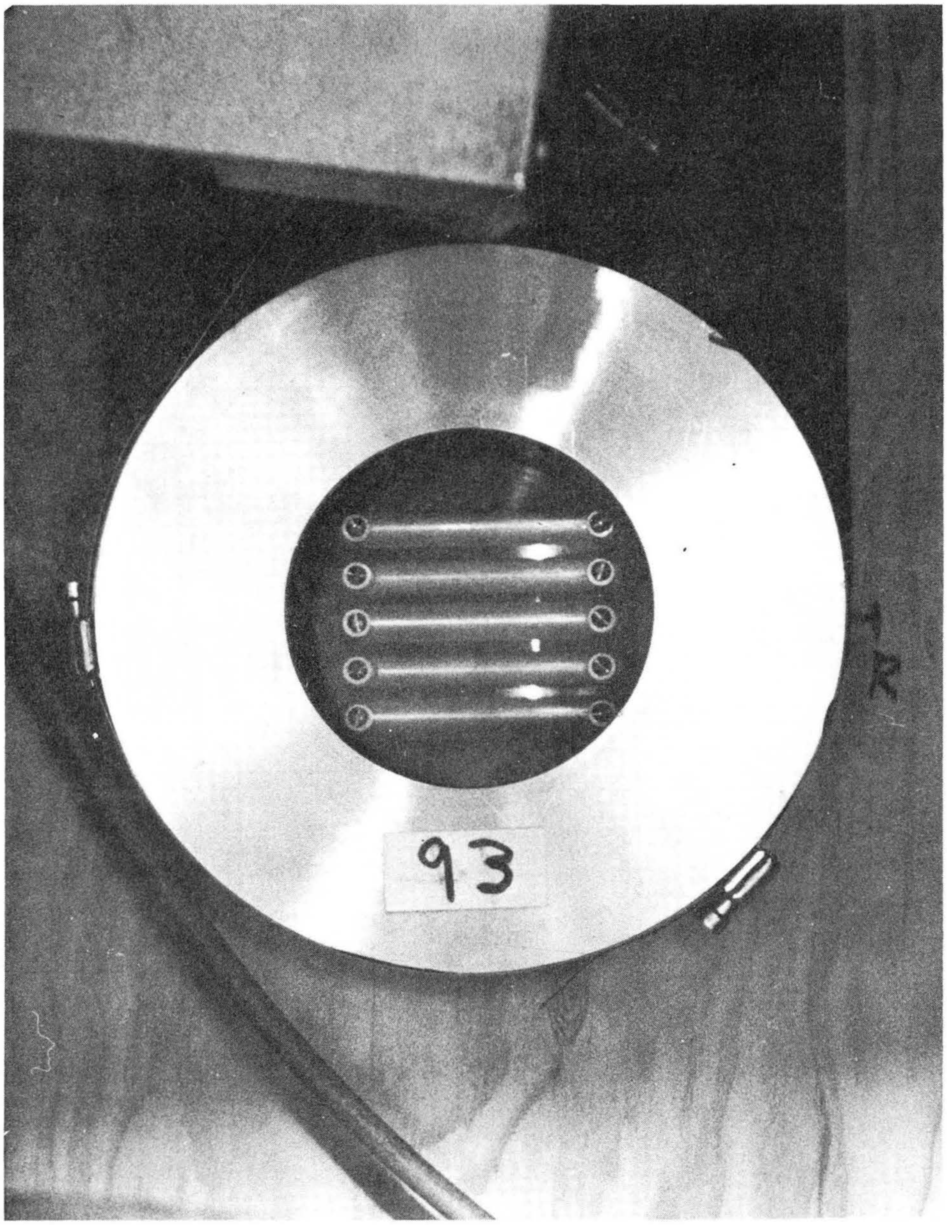

ZN-4789

Fig. 12